Molecular dynamics studies of sluggish grain boundary diffusion in equiatomic FeNiCrCoCu high-entropy alloy

This Accepted Manuscript (AM) is a PDF file of the manuscript accepted for publication after peer review, when applicable, but does not reflect post-acceptance improvements, or any corrections. Use of this AM is subject to the publisher's embargo period and AM terms of use. Under no circumstances may this AM be shared or distributed under a Creative Commons or other form of open access license, nor may it be reformatted or enhanced, whether by the Author or third parties. By using this AM (for example, by accessing or downloading) you agree to abide by Springer Nature's terms of use for AM versions of subscription articles: https://www.springernature.com/gp/open-research/policies/accepted-manuscript-terms

The Version of Record (VOR) of this article, as published and maintained by the publisher, is available online at: https://doi.org/10.1007/s10853-023-08568-3. The VOR is the version of the article after copy-editing and typesetting, and connected to open research data, open protocols, and open code where available. Any supplementary information can be found on the journal website, connected to the VOR.

For research integrity purposes it is best practice to cite the published Version of Record (VOR), where available (for example, see ICMJE's guidelines on overlapping publications). Where users do not have access to the VOR, any citation must clearly indicate that the reference is to an Accepted Manuscript (AM) version.

Molecular Dynamics Studies of Sluggish Grain Boundary Diffusion in Equiatomic FeNiCrCoCu High Entropy Alloy

Axel Seoane, Diana Farkas*, and Xian-Ming Bai*
Department of Materials Science & Engineering,
Virginia Polytechnic Institute and State University

*Corresponding authors. D.F. (diana@vt.edu); X.M.B. (xmbai@vt.edu)

Key words: High entropy alloys; Sluggish grain boundary diffusion; Molecular dynamics simulation.

ABSTRACT

Molecular dynamics simulations are conducted to study the self-diffusion process along an <100>Σ5(210) symmetric tilt grain boundary in a model equiatomic FeNiCrCoCu high entropy alloy (HEA), for the directions both perpendicular and parallel to the tilt axis. For comparison, the grain boundary diffusion process is also quantified for each of the pure components of the HEA. Most importantly, the results are compared with the diffusion along the same grain boundary using the corresponding "average atom" potential that has similar average bulk properties but no compositional randomness as in the HEA. These comparisons show that the self-diffusion in the HEA grain boundary is slower than in the average atom material as well as the average of pure components, suggesting that a "sluggish" diffusion effect exists for this special grain boundary in the HEA. This effect is significant at low temperatures but diminishes at higher temperatures, indicating that the grain boundary sluggish diffusion is likely temperature dependent. Interestingly, the grain boundary sluggish diffusion behavior is different from the bulk diffusion that was studied previously using the same methods and interatomic potentials, in which no significant sluggish diffusion effect was observed. Our further analysis suggests that the combination of the "trapping effect" by compositional complexity in the HEA and the confined 2-D diffusion paths at this special grain boundary is responsible for the observed grain boundary sluggish diffusion.

1. INTRODUCTION

Reliable material performance in extreme environments (e.g., elevated temperature, high stress, harsh irradiation, corrosive condition) is essential to meet the ever-growing demands for energy. High entropy alloys (HEAs) are promising structural material candidates [1, 2] for such applications because they can maintain high strength and phase stability at high temperatures, and may be resistant to radiation damage and corrosion. These unique properties of HEAs may be related to some of their "core" effects [3] including high configurational entropy, distorted lattice, cocktail (mixing) effect, and the possibility of "sluggish diffusion". In particular, the atomic-scale diffusion may play a central role on governing these properties because sluggish diffusion would retard defect and microstructural evolution as well as oxidation kinetics. Sluggish diffusion could be a result of local compositional variation in HEAs, which can create many low-energy sites so that the diffusing elements get trapped [4]. Maximum local compositional variation and thus the configurational entropy is obtained when the elements in equal proportions are randomly distributed in the alloy. The configurational entropy also increases with the increasing number of elements in equiatomic proportions, which can help stabilize the alloy in a single phase if the solution is ideal or close to it (i.e., if the heat of mixing is small). One would logically expect that the more elements in the alloy, the more trapping sites are present and thus the slower diffusion can be achieved. However, more elements do not always lead to slower diffusion experimentally [5, 6]; sometimes simpler alloy compositions can diffuse slower [6, 7]. This result is also confirmed through molecular dynamics simulations of vacancy diffusion in 57 alloys formed from Cu, Ag, Au, Ni, Pd, and Pt [8]. Therefore, the existence of sluggish diffusion in HEAs is still under debate [5, 6, 9]. Even though there is sluggish diffusion reported in the literature for some alloys [1, 5, 6, 9, 10], a significant portion of them depend on if the comparison with pure elements or simpler

alloys is done in the absolute or homologous (T/T_m, where T_m is the melting temperature) temperature scale [9]. The homologous (normalized) temperature scale is used for comparing diffusion at the same vacancy concentrations in the work by Tsai et al. [10], which is the first experimental HEA diffusion measurement. This is important because their CoCrFeMnNi Cantor alloy [11] has a lower melting point than the average of its components. Aiming to provide a more rigorous comparison, recently the present authors [12] conducted molecular dynamic simulations of vacancy diffusion in a bulk FeNiCrCoCu HEA using the embedded atom method (EAM) potential [13] and compared the self-diffusivities with the average of its pure components and most importantly, with its corresponding Average Atom (AA) potential [12, 14]. The AA potential provides a hypothetical element with essentially the same cohesive energy, lattice constant, melting temperature and other properties as the HEA. The key difference is AA's absence of local compositional variation, therefore a lack of configurational entropy, lattice strain and local trapping sites, all of which exist in the HEA. This recent work [12] does not include simulations for simpler alloys, as it is well established that more elements do not lead to more significant sluggish diffusion [5, 6, 8]. Instead, this recent work [12] is focused on the comparison of the HEA vacancy diffusion with the AA vacancy diffusion and found that they have similar bulk selfdiffusivities over a wide range of temperatures, suggesting that vacancy-mediated sluggish diffusion is not evident in the studied bulk HEA. However, it is unclear if this conclusion can be extended to special microstructures containing extended defects, such as grain boundaries.

Grain boundary is a planar defect with some excess volume between two grains. In polycrystalline materials grain boundaries generally serve as highways for mass transport or as nucleation sites for phase transitions. Diffusion along grain boundaries can be order of magnitudes faster than in the lattice [15] and is a principal driving mechanism of sintering, creep, corrosion,

etc. [16-18]. Experimental techniques combined with the Fisher's model [19] or its variations can measure grain boundary diffusion coefficients up to an accuracy of $10^{-22} m^2/s$ [20]. Although grain boundary diffusion has been experimentally measured in many pure metals and simple alloys [21-23], there are very limited studies for HEAs. To the best of our knowledge, there are only two experimental results of grain boundary diffusion in HEAs. The first study [24] used ⁶³Ni isotopes and radiotracer analysis to measure Ni diffusion in both CoCrFeNi and CoCrFeMnNi (Cantor alloy) HEAs. The authors do not claim sluggish diffusion because the Ni diffusion in the 5-element CoCrFeMnNi HEA is faster than that in pure Ni or simpler alloy Fe-40Ni at high temperatures (> 930 K), although Ni diffusion in this HEA is indeed slower at low temperatures. On the other hand, the Ni diffusion in the 4-element CoCrFeNi HEA is always slower than the counterparts in both pure Ni and Fe-40Ni at a wide range of temperatures tested, suggesting that GB diffusion in HEAs could be sluggish. This is also another example that more elements in an HEA do not necessarily mean slower diffusion. It should be noted that the 5-element Cantor alloy has a lower T_m than the Fe-40Ni and pure Ni, which could be the reason why the grain boundary diffusion of Ni in the Cantor alloy is faster at high temperatures in the absolute temperature scale. The second study [25] by the same research group is complementary to the first study [24] as it measures the grain boundary diffusion of other elements in the CoCrFeMnNi Cantor alloy using the same technique. Their results of Co, Cr and Fe in this HEA consistently show slower grain boundary diffusion than their counterparts in pure FCC elements and simpler alloys except for Cr in Ni-10Fe-19Cr, again indicating that sluggish GB diffusion in HEAs is possible.

Although these experiments can provide quantitative values of grain boundary diffusivities, they explain little of the diffusion mechanisms. Most of the knowledge in grain boundary diffusion mechanisms has been obtained through atomistic-scale computational techniques such as

molecular dynamics. Previously, molecular dynamics simulations have been used extensively to study grain boundary diffusion in pure metals and simple alloys [26-28]. When adequate statistics of atomic displacements are collected, molecular dynamics can result in very good agreement with experimental data [29]. Furthermore, this method allows understanding of the specific mechanisms operating in grain boundary diffusion [30] and can take into account the possibilities of the multiplicity of different structures that can arise for the same grain boundary [31]. Using this method, Mishin and co-workers [30, 32] found that grain boundary diffusion mechanisms in pure metals are temperature dependent. At low temperatures, the grain boundary diffusion is controlled by both vacancies and self-interstitials in about the same proportions [30], which is different from lattice diffusion, where vacancies are much more predominant than interstitials. At intermediate temperatures, a fast diffusion event [32] is caused by avalanche-type generation of point defects at irregular intervals followed by the point defects annihilation and a period of slow diffusion. As temperature increases, the avalanches become more frequent until the grain boundary reaches the pre-melting stage. In the pre-melting stage, grain boundary diffusion exhibits a string-like group motion that is similar to the collective atomic motion in supercooled glass-forming liquids [33] or superheated bulk crystals [34] and it deviates from the Arrhenius behavior. It should be noted that molecular dynamics can only directly simulate grain boundary diffusion with enough statistical accuracy at temperatures higher than $0.5T_m$ and up to the pre-melting temperature [29]. This is the temperature range that will be used in this work, as discussed below.

The aim of this work is to use molecular dynamics simulations to elucidate if the grain boundary diffusion in an equiatomic FeNiCrCoCu model HEA can be sluggish, even though its bulk diffusion is not sluggish [12]. The same strategy as in our recent work of bulk diffusion in the HEA [12] will be used: comparing the grain boundary diffusion in the HEA with its AA

equivalent. The former has the compositional complexity while the latter does not. In addition, the average diffusivities of the five pure components will also be compared to that of HEA. As a first attempt, a $\Sigma 5(210)$ symmetrical tilt boundary is used as a model high-angle grain boundary in this work, although more boundaries are needed to be studied in the future to get a complete picture of the grain boundary diffusion mechanisms in HEA. Since molecular dynamics does not require any *a priori* assumption of diffusion mechanisms, it is expected that the diffusion mechanisms of this grain boundary in the HEA will be revealed in this work. The molecular dynamics method also allows for calculations with different starting distributions of the component elements in the grain boundary so that adequate averages can be computed. In addition, it can study grain boundary diffusion in different directions within the grain boundary plane. Moreover, it can help understand the role of vacancies in the diffusion process because some grain boundary sites do not support a stable vacancy. This can be done by comparing results with different vacancy contents in the same grain boundary, which has been done in previous studies [29-31].

2. METHODS

2.1 Molecular dynamics techniques and interatomic potentials: HEA and Average Atom

The molecular dynamics simulations of grain boundary diffusion are performed using a $<100>\Sigma5(210)$ symmetrical tilt grain boundary that contains 9600 atoms. The tilt axis is along the z direction and the grain boundary normal is along the y direction. The dimensions of the grain boundary system in the HEA are about 33Å × 97Å × 36Å. Periodic boundary conditions are employed in all directions so that there are two equivalent grain boundaries in the system. The LAMMPS code [35] is used for all molecular dynamics simulations. The timestep is set to 1fs. The simulations are performed in an NPT (constant number of atoms, pressure, and temperature) ensemble. The Noose-Hoover barostat and thermostat [36] are used to control the external pressure at 0 bar and temperature at the desired values. The EAM [37] interatomic potential used for the FeNiCrCoCu HEA system was developed by one of the present authors - Farkas et al. [13]. This potential predicts the standard deviation of bond lengths for first nearest neighbors up to 2%, a heat of mixing of -0.0002 kJ/mol for the quinary alloy, and the differences in atomic size between components are up to 3%. In addition, all the elements in the potential are set to be stable in the FCC structure in their pure states. Although this potential cannot be expected to predict all the properties in the HEA accurately, it presents an ideal opportunity to study how material parameters affect the alloy properties and to explore the underlying atomistic mechanisms for defect and microstructure evolution processes. For example, this potential has been used to study many atomic mechanisms in the FeNiCrCoCu HEA, including the structure and mobility of dislocations [38], the Hall-Petch effect [39], the temperature effect on plastic inception in uniaxial tension tests [40], and lattice vacancy diffusion [12].

The AA potential (also in the EAM format) averages all the local compositional and structural fluctuations of a random multicomponent alloy to form an averaged single element. This treatment was first done for a model Fe-Ni-Cr alloy by Varvenne et al. [14]. The hypothetical element in the AA potential allows isolating/excluding the role of local compositional variation in the alloy's properties, through the comparisons with its multicomponent counterpart. Recently the present authors [12] followed the method provided in Varvenne's work [14] to develop the AA potential corresponding to the equiatomic FeNiCrCoCu HEA potential [13] and the same AA potential is used in this work. Table 1 shows our previous results [12] of the basic properties predicted by the AA potential, compared with those of the equiatomic FeNiCrCoCu HEA mixture, as well as the average properties of pure components. For completeness, this table is shown here again. It can be seen that the HEA and AA potentials predict very similar properties and they both agree well with the averages of pure components.

It should be noted that currently there is no unique definition of "sluggish diffusion" in the HEA research community. For example, Daw et al. [8] summarized four different criteria of sluggish diffusion. In this work, two comparisons are used to determine "sluggishness". The first one is comparing the HEA and the corresponding AA material. The second one is comparing the HEA with the "rule of mixtures" of the five elemental grain boundary diffusivities (this is one of Daw's criteria). If the HEA grain boundary diffusivities are slower than these reference diffusivities, it is considered as sluggish.

	Average of	Random	Average Atom
	components	HEA	potential
a ₀ (nm)	0.3556	0.3555	0.3554
E _{coh} (eV)	4.20	4.20	4.20
B (GPa)	173	169	189
C ₁₁ (GPa)	214.4	224.8	245.3
C ₁₂ (GPa)	152	140.8	160.8
C ₄₄ (GPa)	105.6	107.9	107.9
$E_{v}^{f}(eV)$	1.44	1.42±0.16	1.43
$E_{v}^{m}\left(eV\right)$	0.98	1.03±0.17	1.03
$T_{m}\left(K\right)$	2047	2070	2130

Table 1: Previous results of the basic properties predicted by the EAM potential for the FeNiCrCoCu HEA mixture, compared with those by the AA potential, as well as the averages of pure component properties [12]. Here a_0 : lattice constant; E_{coh} : cohesive energy; B: bulk modulus; C_{11} , C_{12} , C_{44} : elastic constants; E_v . vacancy formation energy; E_v vacancy migration energy; T_m : melting temperature.

2.2 Calculations of self-diffusivities at grain boundaries

In all grain boundary diffusion calculations, the grain boundary structures are heated from 300 K with an increment of 100 K within 1 ns (1 million steps). Then the temperature is held constant for 10 ns, which allows the observation of the diffusion process. During the isothermal heating stage, a snapshot is taken every 0.1 ns for calculating the GB diffusivity and other analyses. The heating process is repeated until the system reaches 1800 K. At high temperatures, significant changes of the grain boundary structure can happen, such as premelting or a phase change. For example, we have found that for Co at around 1600K the GB disappeared, resulting in a single crystal HCP block. In the case of drastic GB changes, such

as the one mentioned above, the data collection stops. The center of the grain boundary is determined every snapshot by observing two sections along the normal of the grain boundary (y direction): the first section begins around 25 Å to 75 Å which always encompasses the middle grain boundary even if the grain boundary shifts slightly over time and rising temperatures, the second section is from 75 Å to 25 Å where the second grain boundary created by periodic boundary conditions resides. The center of both grain boundaries is obtained by picking the 20 percent of the atoms that had the most grain boundary plane displacement from the last snapshot and averaging their position along the y direction in each section. The grain boundary thickness is estimated to be 1 nm through the potential energy profile across the boundary, as discussed below in the Results section. To calculate the GB diffusivity at each temperature, five independent simulations are performed with different starting velocities and the average diffusivity and standard deviation are reported. In the five simulations, the equiatomic HEA grain boundary structure has not only different initial velocities, but also different random element distributions. Therefore, the statistics contains both ensemble and configurational averages for the HEA grain boundary. The pure grain boundaries (Fe, Ni, Cr, Co, Cu, and AA) are also studied, and the statistics are based on five independent simulations with different initial velocities. To study the self-diffusion process, no vacancies are introduced to the pristine grain boundary. However, it is important to determine if additional vacancies can alter the self-diffusion significantly. In this work, such tests are also performed through adding one vacancy in the grain boundary for both HEA and AA systems. The results show that the additional vacancy does not have a discernible effect on the grain boundary diffusion within the temperature range studied in this work, as discussed below in the Discussion section.

The self-diffusion coefficient (D) at each of the two grain boundary plane directions (x and z) is calculated by tracking the mean square displacement (MSD) $\langle r^2 \rangle$ of the grain boundary atoms in that direction over the time (t) during the 10 ns isothermal heating stage at each temperature,

$$D = \frac{\langle r^2 \rangle}{2t},\tag{1}$$

where the grain boundary atoms are defined as those within the 1nm thickness (δ) of the boundary region. Since the grain boundary thickness is arbitrarily chosen, the diffusivity calculated from Eq. (1) depends on the value of δ . Here the commonly used P (known as triple product) value [24, 41] is reported to account for the grain boundary thickness (δ = 1 nm) and the segregation factor s = 1 as it is for self-diffusion (the concentration is the same in both grain boundary and bulk),

$$P = s \cdot \delta \cdot \mathbf{D}. \tag{2}$$

The criteria for the diffusivities reported in this work are divided into two groups. The first group includes the AA and pure element simulations, where only the diffusivities obtained from a 0.98 R² or better fit of Eq. (1) are reported. Thus, the diffusivities reported for the AA are from 800 K to 1700 K, which begins a little less than 0.5T_m up to the pre-melting temperature range (T_m = 2050 K for the AA). The second group includes the HEA simulations, from which the diffusivities of the HEA and each component are obtained, where its reported diffusivities are the same as the temperature range reported for the AA. This is because comparing the HEA and AA diffusivities, activation energies and preexponential factors in the same temperature range is the fairest comparison. The diffusivity error is obtained through the slopes of the upper and lower worse fits of one standard deviation off the average of the 5 simulations' MSDs for each case [42]. This method for error calculation is used for all Arrhenius figures in this work.

3. RESULTS

3.1 Grain boundary structure

Figure 1a shows a relaxed $<100>\Sigma5(210)$ symmetric tilt grain boundary structure in the FeNiCrCoCu HEA at 0 K, which has a random distribution of its five components. The structure is composed of "kite" structural units as indicated in Figure 1a, similar to those typically found in pure FCC metals [31] as well as that predicted by the AA potential (Figure 1b). The relaxed basic 0 K structures predicted by the potentials are similar for all cases studied. This agreement is consistent with the work by Utt et al. [43], who also found that both HEA and AA models resulted in a similar grain boundary structure. Regarding the excess grain boundary volume, we have calculated that for atoms within 1nm grain boundary thickness. The excess volume per grain boundary atom is about 3.1% of the lattice atom volume for the HEA and 2.7% for the AA at 0 K. So they are similar although the HEA boundary has a slightly larger excess volume, possibly because it has inherently larger distortions (Fig. 2). At higher temperatures, the grain boundary structure can change before significant diffusion occurs at about 600 – 700 K. Specifically, the grain boundary structure with the original "kites" changes to the "split kites" or "filled kites" or combinations of all three structures that were found in Frolov et al.'s work [31]. After significant diffusion begins, the grain boundary structure becomes more distorted. Overall, the distorted grain boundary structures in these systems at higher temperatures are found to be similar. For the purpose of comparing the results between pure components, HEA, and AA material, this is an important requirement. To determine if there is any "sluggish" diffusion effect, the diffusion process must be studied with the same or at least similar grain boundary structure. This study satisfies this requirement.

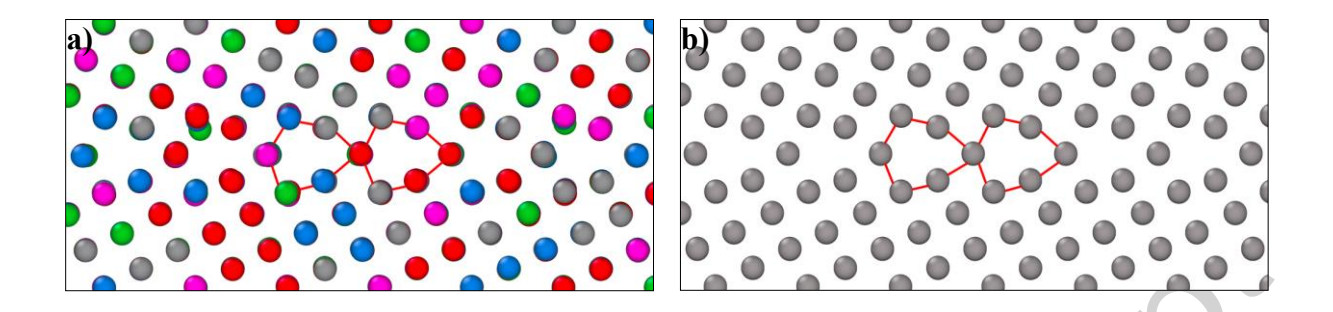


Figure 1. The relaxed $\Sigma 5(210)$ symmetric tilt grain boundary structure at 0 K, a) for the HEA and b) for the AA material, showing "kite" structural units similar to those found in pure FCC metals. Different colored spheres in a) represent different types of atoms in the HEA.

3.2 Lattice distortions

For the bulk HEA, the average lattice distortions (deviation from perfect FCC positions) have been reported to be about 0.07 Å, or about 2% of the lattice parameter [13]. The distortions can be different in the grain boundary region. In order to estimate the differences, we calculated the differences in atomic positions at the relaxed grain boundary regions in the HEA with respect to those predicted by the AA potential, which represents a single element FCC material with the same lattice parameter. The results are shown in Figure 2. Far from the boundary the average distortion values are about 0.07 to 0.08 Å, consistent with the 2% distortion in the bulk HEA, as expected. In contrast, the distortion values in the grain boundary region are significantly higher. In the central boundary plane some atoms have distortions of up to 0.3 Å. More importantly, the distortions are much larger in the two next adjacent planes parallel to the central boundary plane, reaching over 1 Å for some atoms. Figure 2 also shows the distortion values averaged over groups of 200 atoms that have the same distance from the boundary plane. The averaged values in the grain boundary region are about 0.14 Å, twice the average values seen in the bulk. These results clearly show that

the lattice distortions in the HEA are significantly larger in the grain boundary region than in the bulk. This can have important effects on the diffusion behavior along the grain boundary, as discussed later.

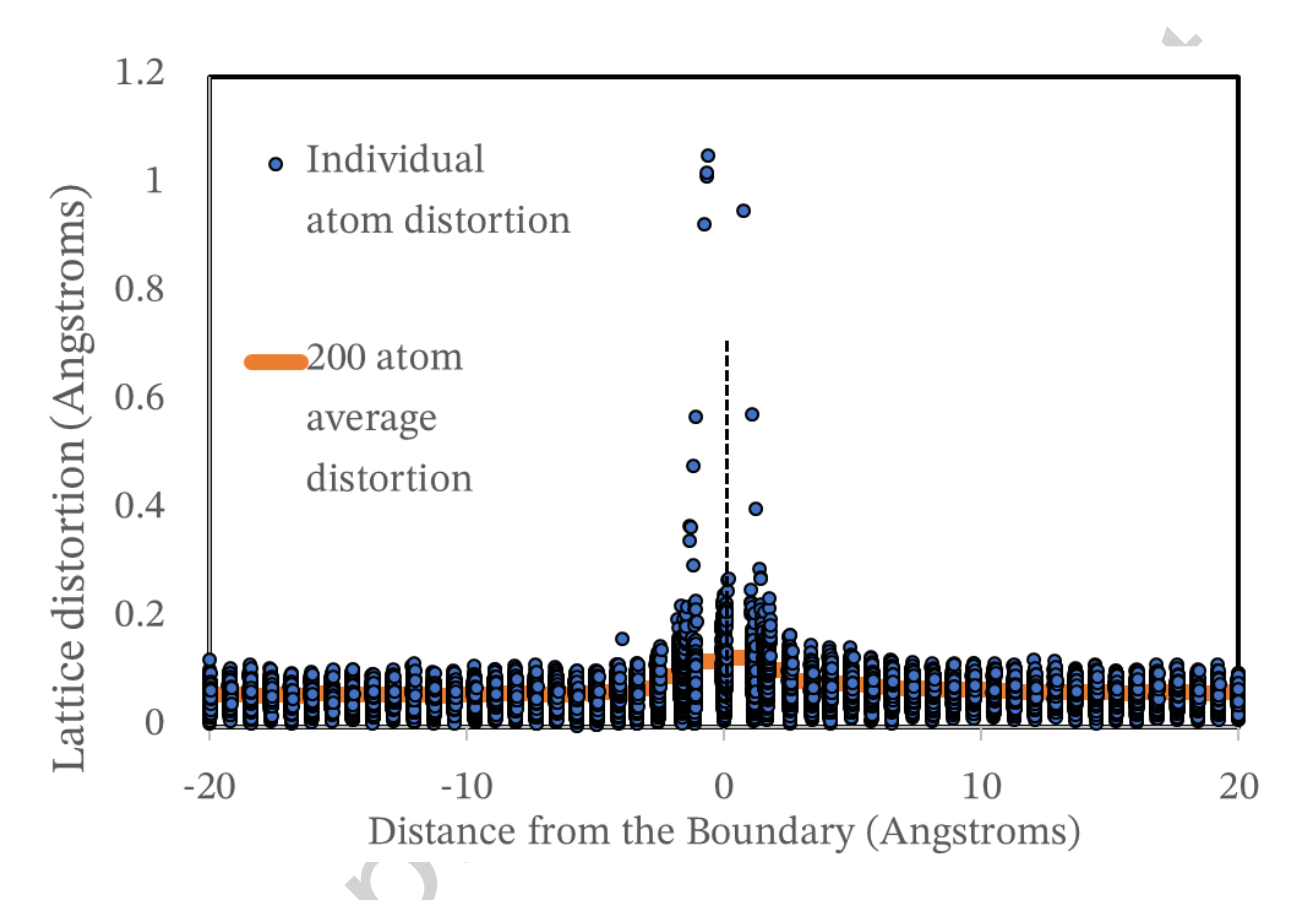


Figure 2. Lattice distortions as a function of distance from the grain boundary plane (dash line). Distortions are calculated as the differences in atomic positions between the relaxed HEA grain boundary structure and those in the single-component FCC material predicted by the AA potential. Distortions are shown for all individual atoms (filled blue circles) as well as averages over 200-atom groups within the same distance to the grain boundary (thick orange line).

3.3 Grain boundary energy and thickness

In order to understand the effects of compositional complexity on grain boundary energy, the grain boundary energies (γ_{GB}) at 0 K are calculated for all individual pure components, the HEA, and the AA material.

The grain boundary energy (γ_{GB}) is calculated with the formula below,

$$\gamma_{GB} = \frac{E - E_{coh} \cdot N_{atoms}}{2 \cdot A_{GB}} \tag{3}$$

where E is the total energy of the bicrystal system at 0 K, E_{coh} is the cohesive energy per atom in a perfect bulk crystal, N_{atoms} is the number of atoms in the bicrystal system and A_{GB} is the area of the grain boundary. The factor of 2 in the denominator accounts for the two equivalent grain boundaries formed in the bicrystal system due to the periodic boundary conditions. The results are shown in Figure 3, where the grain boundary energies are plotted as a function of the cohesive energy. Clearly, the grain boundary energies for the chosen boundaries scale nearly linearly with the respective cohesive energies for all pure components, HEA, and AA material. The AA value is very close to the average of the pure components, while the HEA grain boundary energy is almost identical to the average value of pure components. Note that by design the AA material has the same cohesive energy as the HEA, and thus their corresponding grain boundary energies are very similar. When considering the individual pure components, their cohesive energies vary and so do the grain boundary energies. Overall, the grain boundary energies in these systems follow the same trend as the bulk cohesive energies.

In order to determine the grain boundary thickness, Figure 4 shows the potential energy profiles of atoms across the grain boundary plane for both HEA and AA material at two different temperatures: 900 K and 1700 K. Figure 4 is done by averaging the potential energy per atom over groups of atoms every 2 Å along the y axis (perpendicular to the boundary plane) from 20 Å up to 80 Å position in the bicrystal, which encompasses the middle grain boundary only. Therefore, only

the thickness of the middle grain boundary is measured, while the second grain boundary created by the periodic boundary conditions is assumed to have the same thickness. For clarity, the profile is plotted from its distance from the boundary plane (defined at 0 nm). The largest peak in each potential energy profile corresponds to the grain boundary region and its width can be used to quantify the grain boundary thickness. The HEA and AA material have a similar grain boundary thickness, which is about 1 nm for both systems at both temperatures. However, the main difference in the profile between HEA and AA material is that the former has larger fluctuations in the bulk region (i.e., away from the boundary) due to the compositional variation and thermal noise, while the later has much smaller variations due only to the thermal noise. The results demonstrate that the grain boundary thickness does not significantly vary with temperature or material. Therefore, in this work, the thickness of the grain boundary is defined as 1 nm for all temperatures and materials studied, which is used for the δ value in Eq. (2). Overall, from Figures 1, 3, and 4, it can be seen that the HEA and AA models predict similar grain boundary structures, energies, and thicknesses. Therefore, even though the AA model was developed for matching the bulk properties of HEA, it shows a good transferability for predicting the GB structure and energetics.

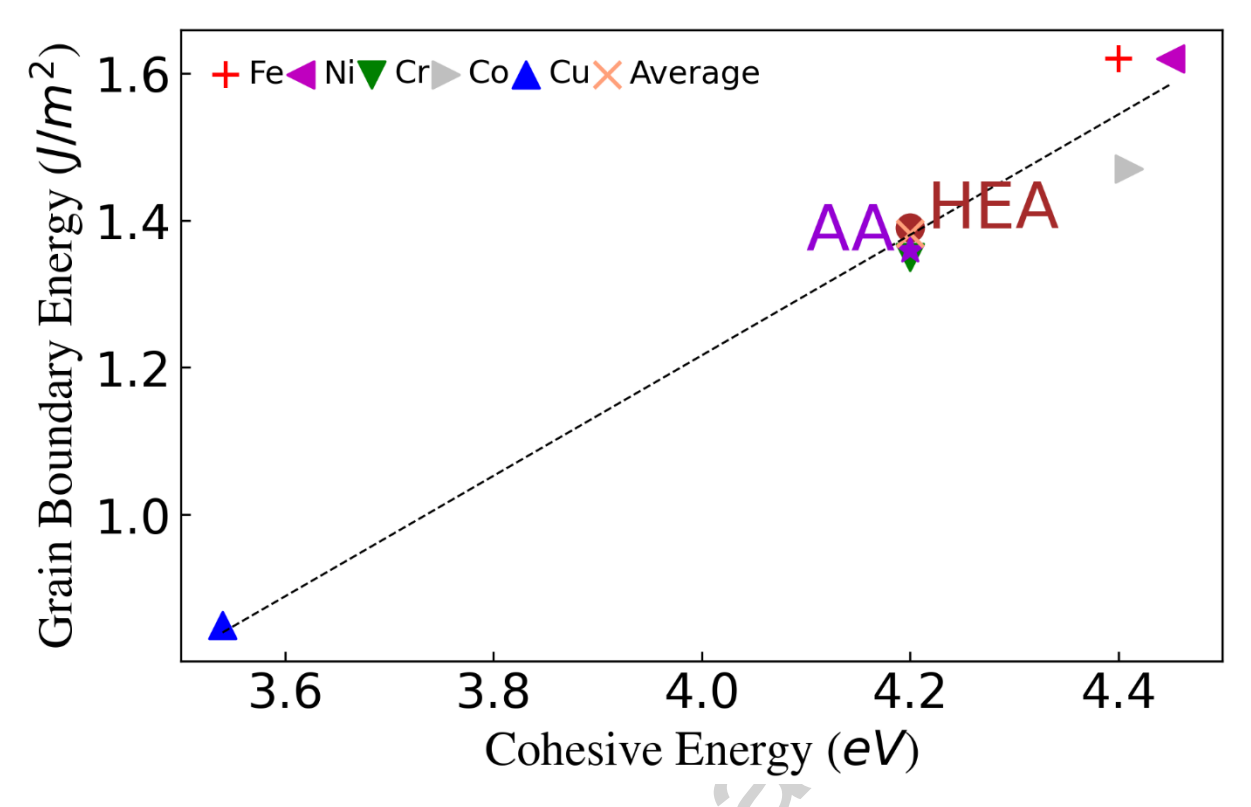


Figure 3. Correlation of the grain boundary energy with the cohesive energy for the five individual pure components, the HEA mixture, and the AA material.

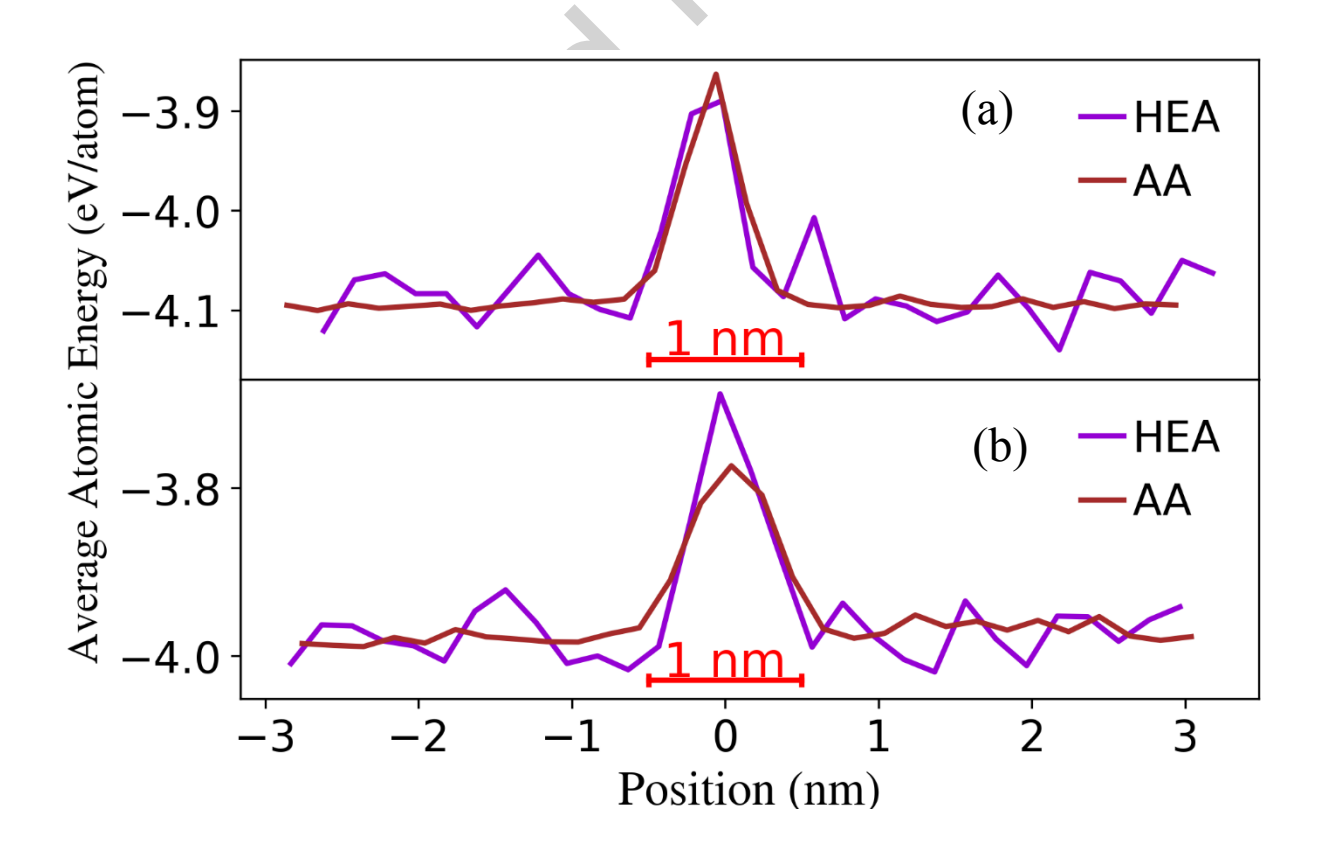


Figure 4. Average potential energies of atoms as a function of distance from the grain boundary plane (at 0 nm) in the HEA and AA material at a) 900 K and b) 1700 K. The GB thickness is determined to be about $\delta = 1$ nm for all cases.

3.4 Grain boundary diffusion in HEA and AA material

To obtain the grain boundary self-diffusivities, the mean square displacements of the atoms within 1 nm thickness of grain boundary region are tracked at each temperature. Figure 5 shows the results of mean square displacements of these grain boundary atoms as a function of time for the HEA and AA material at the five highest temperatures (1300 – 1700 K). The mean square displacements in the two in-plane directions parallel (\parallel , which is along the z direction) and perpendicular (\perp , which is along the x direction) to the rotational axis are plotted separately to understand the grain boundary diffusion anisotropy, if any. From these plots, it can be seen that the AA material results in faster diffusion in both in-plane directions because their slopes are steeper than the counterparts in the HEA.

From the atomic displacement results, Equations (1) and (2) are used to calculate the D and P values for the grain boundary self-diffusion in the HEA and AA material. Then the Arrhenius plots of P values are constructed, as shown in Figure 6. In addition, the grain boundary self-diffusivities in all five pure components are also calculated (more details are provided in the following section) and their averaged values are shown in Figure 6 for comparison. Here the averages of the pure components (i.e., rule of mixtures) are obtained by averaging the activation energies and preexponential factors of the pure components, respectively. The corresponding preexponential factors (P₀) and activation energies (Q) for the HEA, AA material, and average of pure components are reported in Table 2. Figure 6 shows that the AA material has similar grain boundary diffusivities as the average of pure components over a wide range of temperatures, especially in

the in-plane direction parallel to the rotation axis (Figure 6b). However, both of them have higher diffusivities than the HEA and the differences become more evident at low temperatures. Therefore, the results show sluggish grain boundary diffusion behavior that is pronounced at low temperatures but vanishes at high temperatures. The presence of sluggish grain boundary diffusion in the HEA is in clear contrast to the non-sluggish diffusion behavior in the bulk HEA as the present authors found recently [12], using the same interatomic potentials as in this work. Note that the temperature dependence of the grain boundary sluggish diffusion has also been observed experimentally for the CoCrFeMnNi HEA [24], in which sluggish diffusion is observed at 800 K (e.g., $D_{Ni}/D_{CoCrFeMnNi} \approx 2$) while the trend is reversed ($D_{CoCrFeMnNi} > D_{Ni}$) above 950 K. Since diffusivity decreases exponentially with temperature, it is expected that the higher activation energy in the HEA (Table 2) will induce a more pronounced sluggish diffusion at even lower temperatures such as the room temperature. From Table 2, it also can be seen that the two in-plane directions have similar activation energies and preexponential factors in each material, indicating that the diffusion anisotropy is not significant in these grain boundaries.

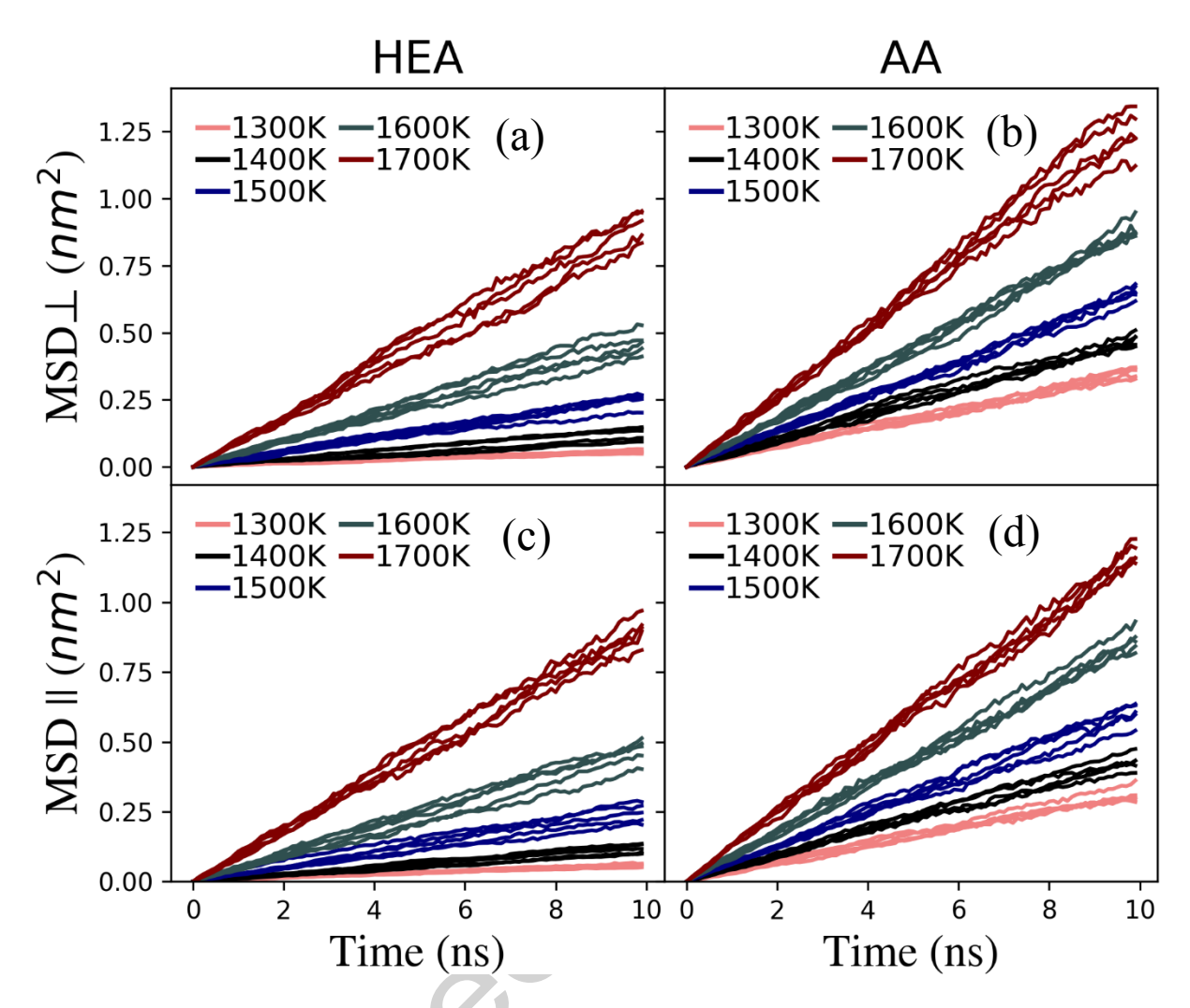


Figure 5. Mean square displacements (MSD) as a function of time for the HEA (a and c) and the AA material (b and d) at different temperatures from 1300 - 1700 K. Here "MSD \perp " and "MSD \parallel " represent the in-plane mean square displacements perpendicular and parallel to the rotation axis, respectively. At each temperature, the five lines represent five independent runs that are used for statistics.

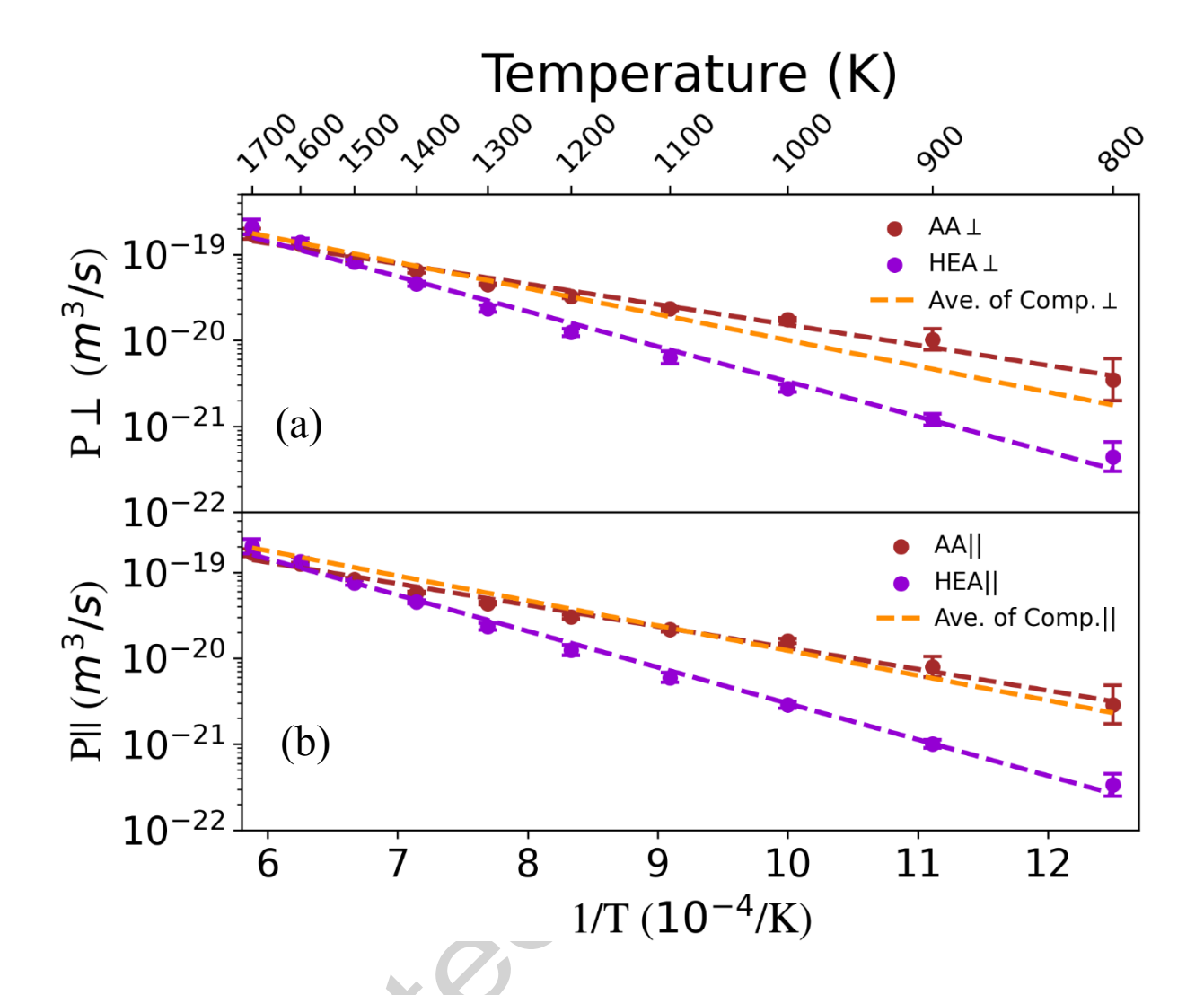


Figure 6. Arrhenius plots of the grain boundary diffusion in the HEA and AA material in both the (a) perpendicular (\perp) and (b) parallel (\parallel) directions to the rotation axis. The averages of five pure components are also shown in each figure. Compared to the AA material and the average of pure components, the "sluggish" diffusion in the HEA is evident at low temperatures but diminishes at high temperatures. Some error bars are invisible because they are smaller than the symbol size.

			Ave. of Pure
	AA	HEA	Components
Q ⊥ (kJ/mol)	45	78	58

Q ∥ (kJ/mol)	48	81	56
$P_0 \perp (\text{m}^3/\text{s})$	3.56E-18	3.99E-17	1.05E-17
$P_0 \parallel (\text{m}^3/\text{s})$	4.08E-18	4.80E-17	9.78E-18

Table 2. Activation energy (Q) and preexponential factor (P_0) of the grain boundary diffusion in both in-plane directions for the AA material, HEA, and the average of pure components.

3.5 Diffusion behavior in the pure component grain boundaries

The grain boundary self-diffusivities in all five pure components are also calculated using the same approach as in the previous section. Since these pure components in the FCC phase have different melting temperatures, the temperature ranges for studying the diffusion are also different (especially for Cu as its melting temperature is the lowest) and the reported diffusivities meet a criterion of 0.98 R² or better fit of Eq. (1). The Arrhenius plots of P for these pure components in the two in-plane directions are shown in Figure 7. The results of the AA material are also included for comparison. Table 3 reports the preexponential factors and activation energies of these pure components from the Arrhenius fits. Note that Figure 7 only shows the diffusivities where the fit of the mean square displacement over time is 0.98 R² or better, hence the value of Fe at 1100 K is missing.

Figure 7 shows that the grain boundary diffusivities in these pure components have large differences. In general, the diffusivities in both in-plane directions follow the trend: $D_{Fe}^{GB} < D_{Ni}^{GB} < D_{Co}^{GB} < D_{Cr}^{GB} < D_{Cu}^{GB}$. This trend of grain boundary diffusion is similar as that observed for vacancy-mediated bulk or lattice diffusion in these pure components obtained using the same potential: $D_{Fe}^{bulk} < D_{Ni}^{bulk} < D_{Co}^{bulk} \approx D_{Cr}^{bulk} < D_{Cu}^{bulk}$ [12]. In both grain boundary diffusion and bulk diffusion,

Cu has a significantly higher diffusivity than other components at the same temperature. Regarding the anisotropy of grain boundary diffusion, Ni, Cr and Co essentially have no anisotropy in the two in-plane directions, as can be seen from the preexponential factors and activation energies shown in Table 3. Fe and Cu have a slight diffusion anisotropy, with slightly faster diffusion (or lower activation energy) in the direction parallel to the rotation tilt axis, as shown in Table 3.

Out of the five HEA elements, only Ni and Cu are naturally FCC and can easily be compared with other molecular dynamic studies of the same grain boundary. Mendelev et al. [28] reported that the activation energy of a $\Sigma 5$ grain boundary diffusion in Ni varies significantly with its inclination, ranging from 50 to 110 kJ/mol, and our values for Ni lie within that range (Table 3). Frolov and Mishin [44] calculated the activation energy of a $\Sigma 5$ grain boundary diffusion in Cu as 0.48 eV or 46 kJ/mol, which is higher than our 30 kJ/mol in-plane average result. However, the discrepancies may be due to a different interatomic potential used in their work. In reality, Fe does turn into FCC in the high temperature range (≥ 1200 K), but the present authors could not find any self-diffusivity studies for the $\Sigma 5(210)$ grain boundary in an FCC Fe for comparison.

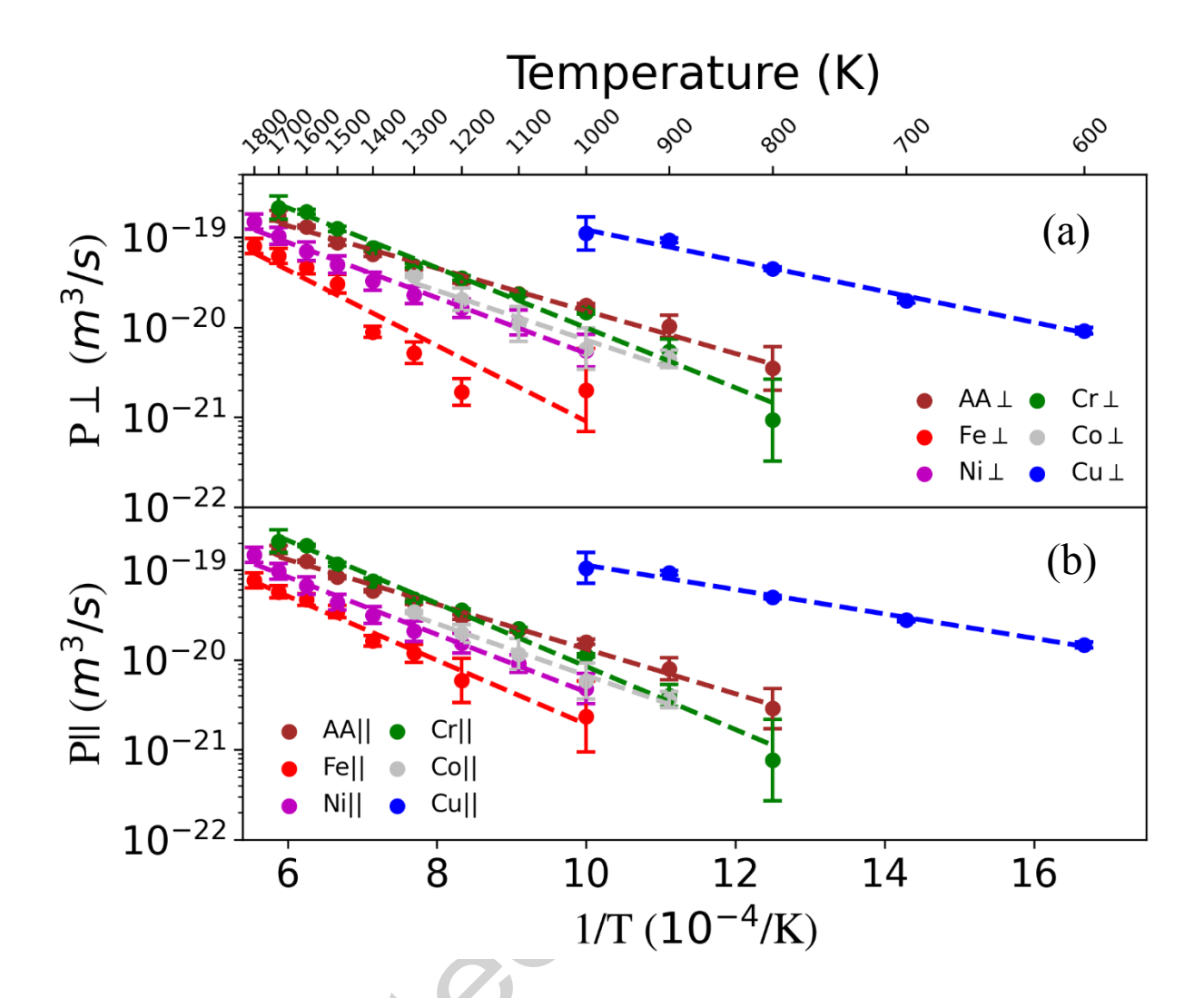


Figure 7. Arrhenius plots of the grain boundary diffusion of the five pure components in the two in-plane directions. The results of the AA material are also shown for comparison. Some error bars are invisible as they are smaller than the symbol size. (a) The direction perpendicular (\bot) to the rotation axis. (b) The direction parallel (\parallel) to the rotation axis.

	Q(kJ/mol)	$P_0 \ (m^3/s)$
Fe ⊥	81	1.45E-17
Fe	68	7.06E-18
Ni ⊥	59	6.27E-18

Ni	61	7.01E-18
Cr ⊥	64	2.14E-17
Cr	67	2.73E-17
Со⊥	53	4.08E-18
Co	55	5.02E-18
Cu ⊥	33	6.31E-18
Cu	26	2.56E-18

Table 3. Activation energies (Q) and preexponential factors (P_0) for the two in-plane directions of grain boundary diffusion in five pure components.

3.6 Diffusion behavior of five individual components in the HEA grain boundary

The mean square displacements of each of the five individual components in the HEA grain boundary region are also tracked and their respective diffusivities are calculated. The Arrhenius plots of these components are shown in Figure 8. Compared to the very scattered diffusivities in pure-component grain boundaries (Figure 7), these components have more similar diffusivities in the HEA. The component diffusivities follow the order: $D_{Fe}^{HEA} < D_{Ni}^{HEA} \approx D_{Co}^{HEA} \approx D_{Cr}^{HEA} < D_{Cu}^{HEA}$. In particular, Cu is still the fastest diffuser at every temperature as in pure components (Figure 7), but the differences between Cu and other components are much smaller in the HEA than in the pure components. In comparison with the AA material, all the components in the HEA have lower diffusivities at temperatures below 1200 K in both in-plane directions.

Table 4 shows the activation energies and preexponential factors for all HEA components at the two in-plane directions. In comparison with the results of pure-component grain boundaries (Table 3), all the activation energies in the HEA, with the exception of Fe along the perpendicular

direction, are higher than the counterparts in the pure components although all the preexponential factors are also higher. In particular, the activation energy of Cu averaged over two directions increases about 2.6 times from the pure Cu value. In addition, all components have similar activation energies along the two in-plane directions, unlike the anisotropy seen for pure Fe and Cu (Table 3). Overall, the results indicate that the diffusivities of the individual components in the HEA are more similar than the large differences observed between pure components.

Since there are no experimental results for the FeNiCrCoCu HEA grain boundaries, the experimental grain boundary diffusion results in a similar HEA in which Cu is replaced with Mn, CoCrFeMnNi [25], are used for comparison with our modeling results, as shown in Table 4. Clearly, the activation energies of HEA components calculated in this work are much lower (more than 2 times) than the experimental values. On the other hand, the experimental preexponential factors are much higher. In a four-component CoCrFeNi HEA (without Cu or Mn), the experimentally measured activation energy of grain boundary diffusion is about 158 kJ/mol [24], while the calculated overall activation energy in our CoCrFeNiCu HEA is 80 kJ/mol (Table 2). The calculated activation energies from our simulations are smaller than those measured from experiments. There could be a few reasons for the discrepancies. First, the FeNiCrCoCu HEA studied in this work contains Cu, which is a faster diffuser and likely reduces the overall activation energy. Second, the experimental HEA may contain some impurities, which could slow the diffusion kinetics and increase the activation energy. In contrast, the HEA studied in this work is impurity free. Third, the activation energy calculated in this work is from a single $\Sigma 5(210)$ symmetric tilt grain boundary, while the experimental value is the average of different types of grain boundaries. The grain boundary diffusion is sensitive to the details of boundary structure. For example, in a previous molecular dynamics simulation [28] it is reported that the activation

energy for the $\Sigma 5$ grain boundary diffusion in Ni varies significantly with its inclination, ranging from 50 to 110 kJ/mol.

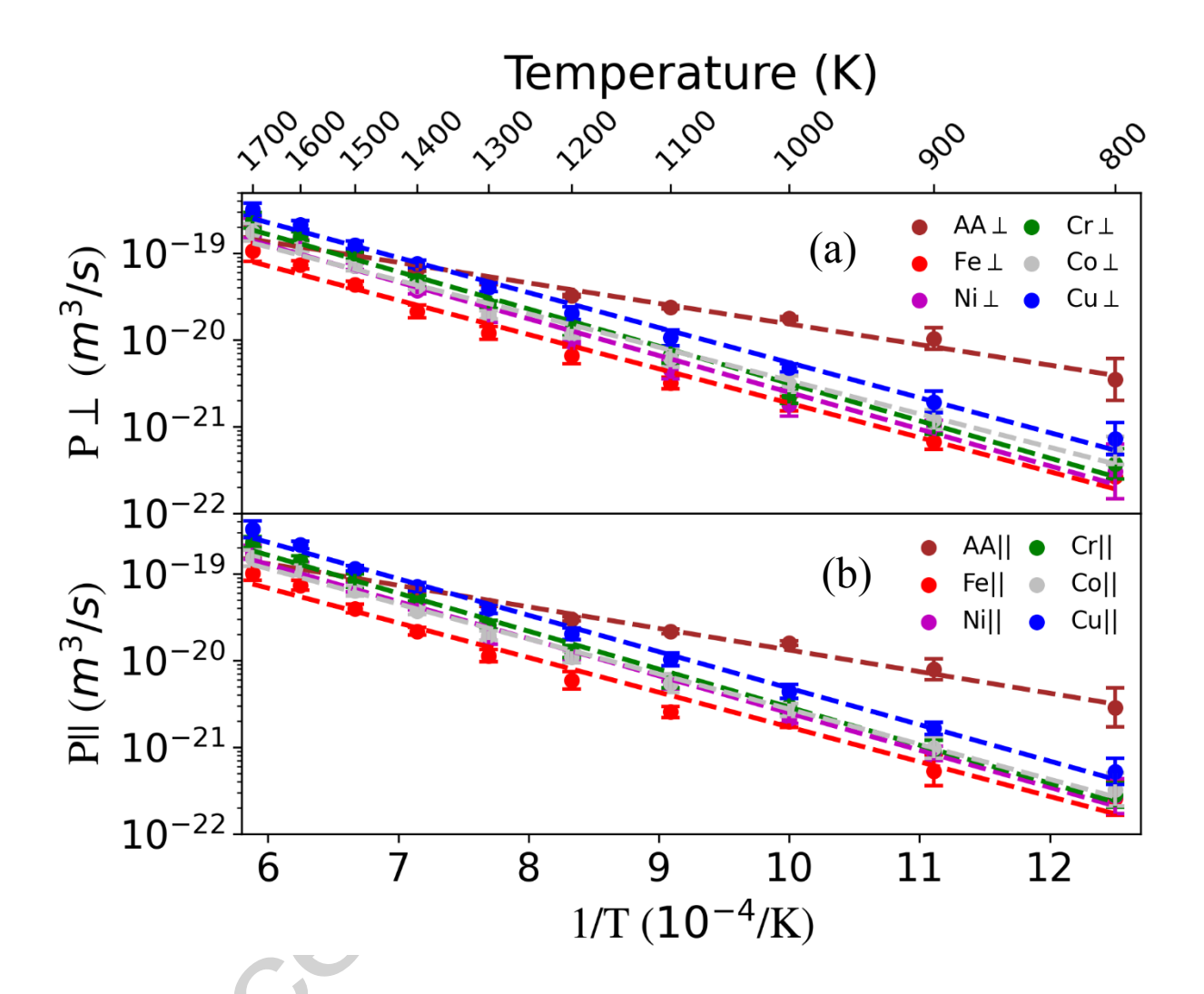


Figure 8. Arrhenius plots of the diffusion of five individual components in the HEA grain boundary. The results of the AA material are also included for comparison. Some error bars are invisible because they are smaller than the symbol size. (a) The direction perpendicular (\bot) to the rotation axis. (b) The direction parallel (\parallel) to the rotation axis.

	Q (kJ/mol)	P_0 (m ³ /s)	Exp. Q (kJ/mol) in	Exp. P_0 (m ³ /s) in
	(this work)	(this work)	CoCrFeMnNi GB [25]	CoCrFeMnNi GB [25]
Fe ⊥	76	1.68E-17	182.2	1.40E-12
Fe	77	1.73E-17		1. 4 0L-12
Ni ⊥	81	4.33E-17	221	1.42E-10
Ni ∥	82	4.79E-17	221	1.4212 10
Cr ⊥	82	6.24E-17	180.6	1.43E-12
Cr	84	7.01E-17	100.0	1.43L-12
Со⊥	74	2.40E-17	181.5	1,66E-12
Со∥	77	3.06E-17	101.5	1.00E 12
Cu ⊥	77	5.95E-17		
Cu	81	7.72E-17		

Table 4. Activation energies (Q) and preexponential factors (P₀) of the five components in the HEA grain boundary along the two in-plane directions. The experimental results of a similar HEA in which Cu is replaced by Mn, CoCrFeMnNi [25], are included for comparison.

4. DISCUSSION

The primary purpose of this work is using molecular dynamics simulations to study if grain boundary diffusion in HEAs can be sluggish, through comparing the self-diffusivity in an $<100>\Sigma5(210)$ symmetric tilt grain boundary between an equiatomic FeNiCrCoCu HEA and its corresponding AA material. This comparison is ideal because the AA potential models a hypothetical single element, which predicts the average equilibrium properties of all components in the HEA but lacks the effects from compositional randomness present in the HEA. Therefore, the obtained diffusivity from the AA potential is expected to be close to the average of the five pure components, and this is indeed the case as shown in Figure 6. In contrast, the grain boundary

diffusion in the HEA shows a clear sluggish diffusion behavior in comparison with the AA material and the rule of mixtures of pure components, and the sluggish effect is more pronounced at low temperatures but diminishes at higher temperatures (Figure 6). Since the AA potential represents a hypothetical single element, there is no experimental equivalent for this comparison. The current literature [7, 24, 25] compares the HEA diffusivity with pure elements or simple binary or ternary alloys which excludes some of the elements used, because it is difficult to have all the elements in an FCC structure at the tested temperatures for a fair comparison. It should be noted that our recent study [12] of lattice diffusion using the same methods and interatomic potentials did not show a sluggish effect in the bulk HEA. To summarize the difference in sluggish diffusion between this specific grain boundary and bulk, Figure 9 shows the grain boundary results obtained in the present work, together with those obtained for bulk lattice diffusion reported in our recent work [12]. As expected, grain boundary diffusion is characterized by significantly lower activation energies than the bulk diffusion. Most importantly, in comparison with the reference AA material, the HEA lattice diffusion is not sluggish at any temperature (in fact it is slightly enhanced) while the HEA of this special grain boundary diffusion is clearly sluggish at low temperatures. In order to explore the possible reasons for the sluggishness in grain boundary diffusion, two approaches are pursued: first the role of vacancies in the diffusion process is studied and second the examination of the diffusion paths along the grain boundary is conducted.

The reason for exploring the role of vacancies is that the non-sluggish diffusion in the bulk HEA is vacancy-driven in the simulation, while the sluggish grain boundary diffusion in this work is obtained without introducing any extra vacancies. To address this point, we repeat the grain boundary diffusion simulations, one for the HEA and one for the AA, with an initial vacancy introduced in each grain boundary. The results are compared to those without extra vacancies

(Figure 6), as shown in Figure 10. The comparison reveals no significant difference caused by the presence of a vacancy, at least in the temperature range studied (900 – 1700 K), and the sluggishness at low temperatures is still present after the vacancy is introduced. Therefore, it is concluded that the HEA diffusion at this grain boundary is at least not purely driven by the vacancy hopping mechanism as in the lattice. This is reasonable, since it is known that the grain boundary diffusion mechanisms are complex [29, 30, 32]. The excess volume of the grain boundary allows the atoms to diffuse along the boundary without the need of extra vacancies. The process in the case of lattice diffusion is vacancy driven and this difference may help explain why sluggishness was not observed in the bulk but is observed in the grain boundary case.

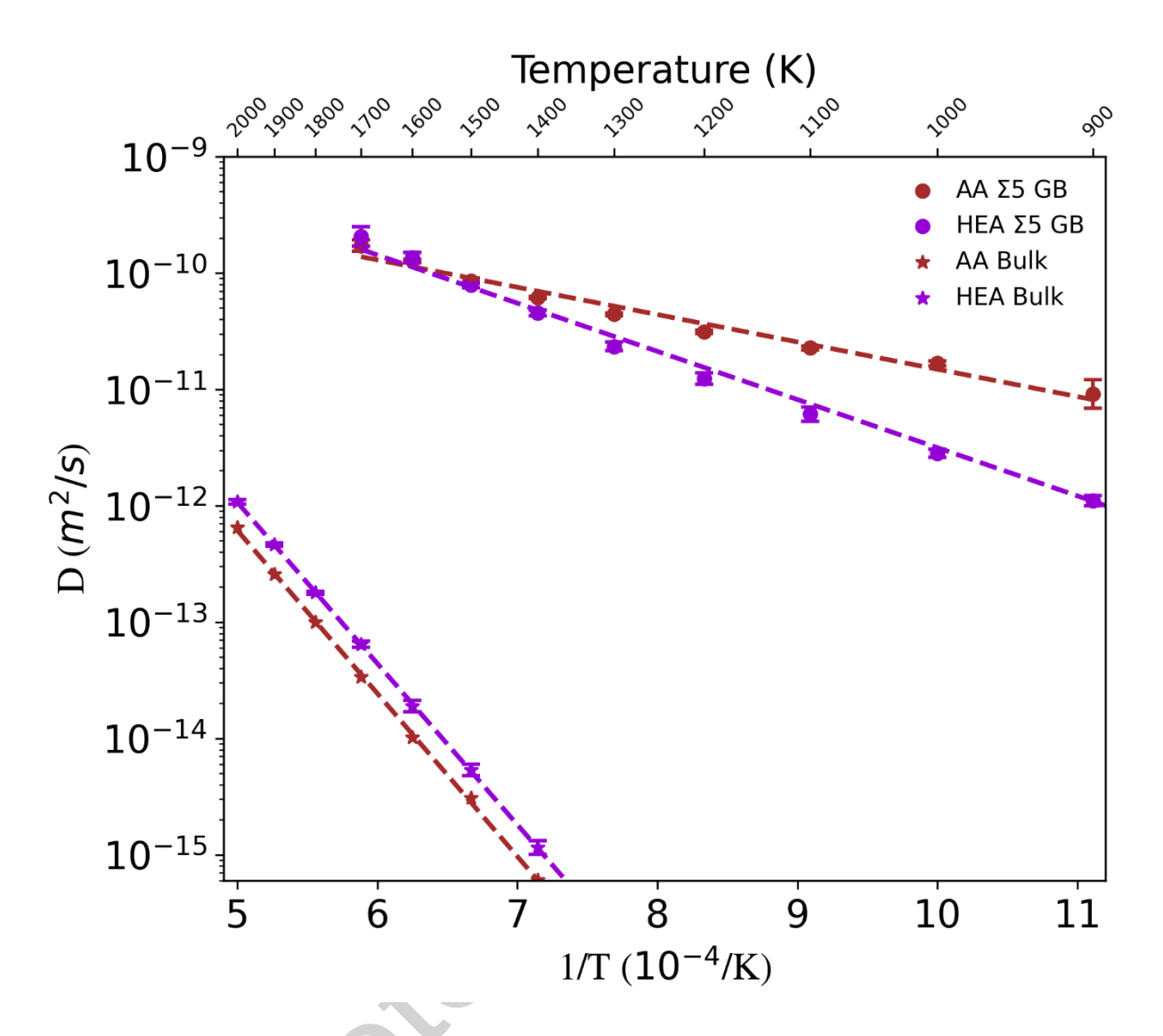


Figure 9. Arrhenius plots of the total grain boundary (this work) and bulk self-diffusivities ([12]) in the FeNiCrCoCu HEA compared to those in the AA material. To compare them in the same figure, the D values rather than P values are used for the total grain boundary diffusivities.

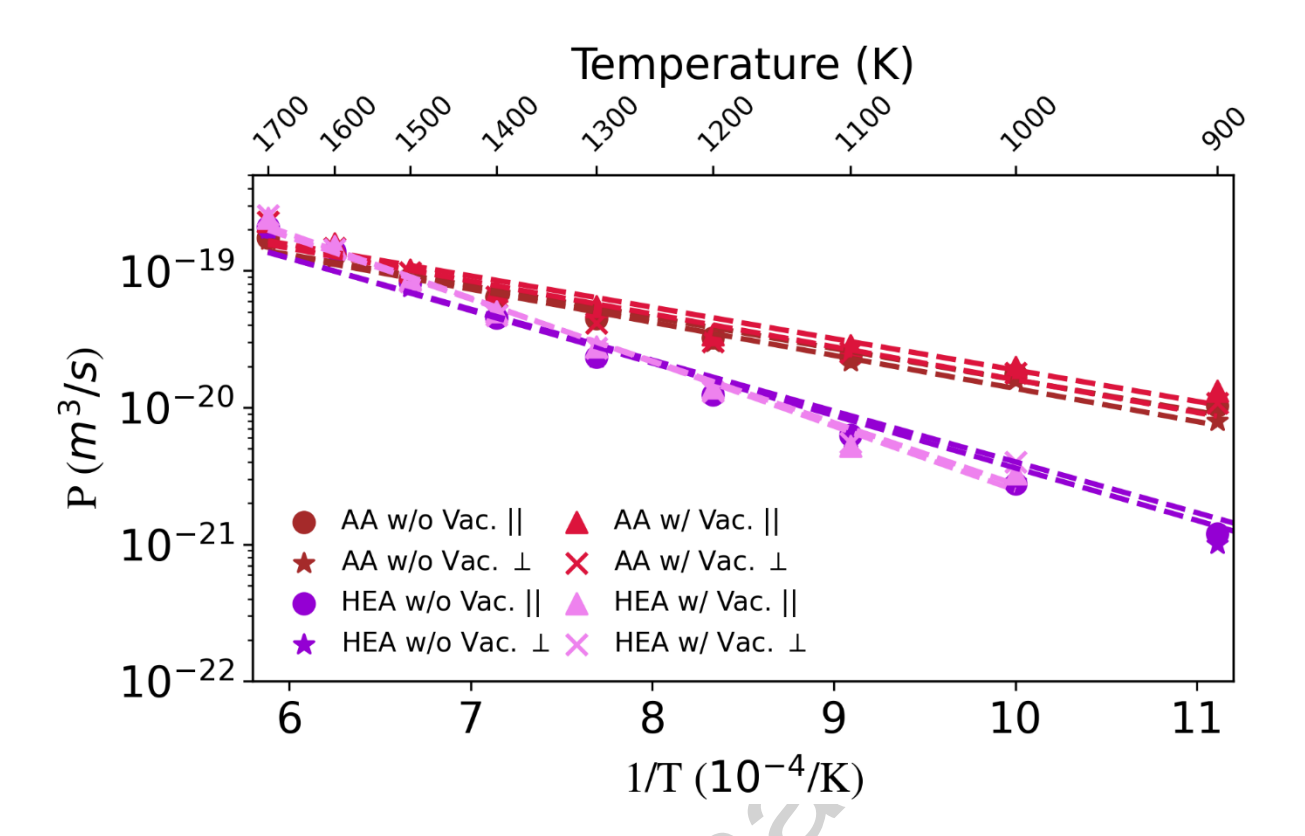


Figure 10. Arrhenius plots of the diffusivities with (w/) and without (w/o) an extra vacancy at the grain boundary in the HEA and AA material along the two in-plane directions.

To further understand the results, the details of grain boundary diffusion mechanisms are studied for both HEA and AA material. This is achieved by tracking the atom trajectories during the diffusion process to examine the atom diffusion paths. Here the atom trajectories during a time period of 1 ns are analyzed using the OVITO software [45] for both systems at a low temperature (900 K) and a high temperature (1600 K), as shown in Figures 11 and 12, respectively. The corresponding grain boundary structures are also shown. At 900 K, the grain boundary diffusion paths lie mainly along the central boundary plane. However, in the HEA case the paths are seen to circumvent the central plane in some places, showing diffusion outside of the central boundary region (Figure 11b). In contrast, the diffusion paths in the AA boundary have routes along the

central boundary plane and the two adjacent planes, with no jumps outside the grain boundary region. (Figure 11d). The different diffusion routes between HEA and AA suggest the important role of compositional complexity on the grain boundary diffusion. Compositional randomness of components can induce many trapping (low energy) sites [12]. These trapping effects at the HEA grain boundary may be even stronger because the grain boundary has significantly large lattice distortions than in the bulk HEA, as shown in Figure 2. Since a grain boundary is also a defect sink [46], the energy cost for the components to diffuse out of the central boundary plane is expected to be high. Given that a grain boundary has a 2D geometry, the presence of trapping sites can inhibit the in-plane diffusion along the grain boundary, forcing higher energy jumps away from the grain boundary region. As a result, atom diffusion has to go through some alternative but energetically expensive routes outside of the central boundary plane, as shown in Figure 11b. In the AA material in which no such composition-induced trapping sites exist, atoms diffuse mainly along the faster boundary plane at low temperatures, as shown in Figure 11d. At high temperatures (e.g., 1600 K) when the kinetic energies are sufficiently high, more atoms in the HEA can overcome the trapping sites through both in-central-plane and out-of-central-plane diffusion, as shown in Figure 12b. The out-of-central-plane diffusion also happens at the AA grain boundary at this temperature, as shown in Figure 12d. Therefore, both HEA and AA grain boundaries end up with similar diffusion mechanisms at high temperatures. This is likely the reason why the HEA and AA have different grain boundary diffusivities at low temperatures but similar ones at high temperatures.

This analysis of the diffusion paths may explain why diffusion is sluggish at this HEA grain boundary but not in the bulk HEA (see Figure 9). The key difference is that the bulk diffusion is in 3D while grain boundary diffusion is 2D. In the 3D bulk diffusion, atoms have many alternative

paths to "escape" or "bypass" the trapping sites. For example, there are twelve nearest neighboring paths for a vacancy-mediated diffusion in the bulk FCC crystal. However, for the 2D grain boundary diffusion, the "trapping" sites can effectively inhibit the in-plane diffusion due to the limited number of paths in the confined 2D space, causing a "traffic" or "blocking" effect. The atoms may have to diffuse out of the boundary plane (Figure 11b) to escape from the trapping sites, which needs to overcome high-energy barriers due to the grain boundary segregation effect. Therefore, the sluggish effect is significant for this HEA grain boundary diffusion and the effect is pronounced at low temperatures, while such effect is not evident in the bulk HEA.

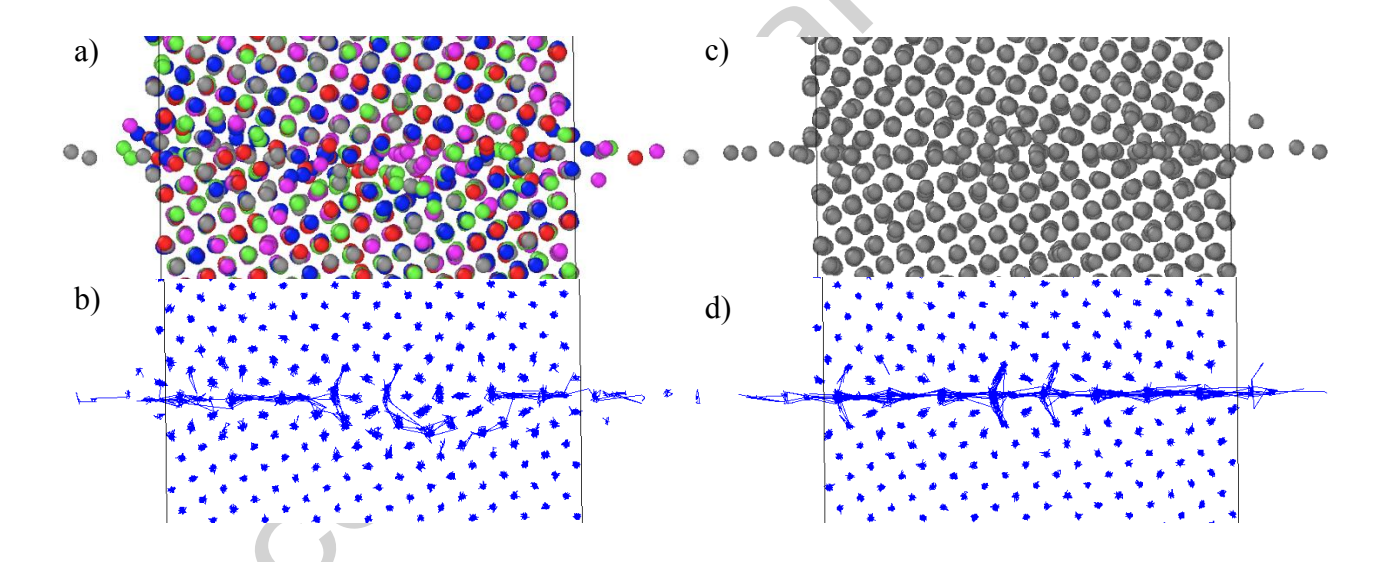


Figure 11. Grain boundary structures and diffusion trajectories at 900 K for the HEA (a - b) and AA material (c - d). The sphere colors in (a) represent different types of atoms in the HEA. Note that at this low temperature, the diffusion paths in the HEA can jump out of the grain boundary region while those in the AA material are mainly along the central boundary plane. This explains why the sluggish diffusion effect in the HEA is significant at low temperatures.

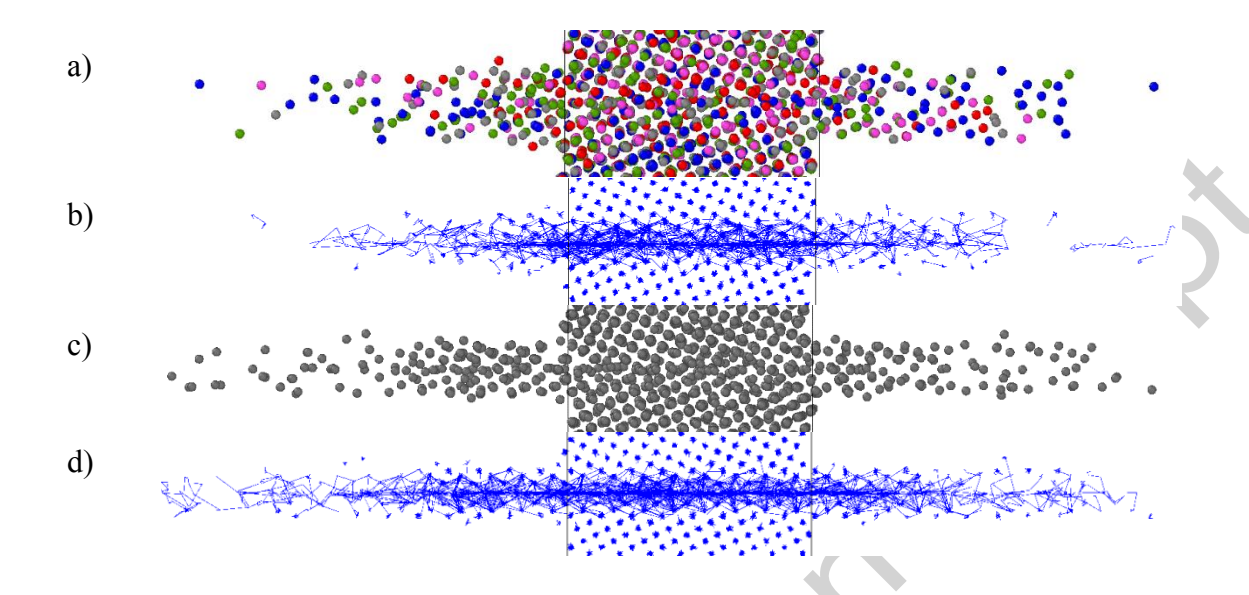


Figure 12. Grain boundary structure and diffusion trajectories at 1600 K for the HEA (a - b) and AA material (c - d). The sphere colors in (a) represent different types of atoms in the HEA. Note that at this high temperature, the diffusion paths in both HEA and AA boundaries are similar. As a result, the sluggish diffusion effect vanishes at high temperatures.

As mentioned in the Introduction, this work only focuses on a $\Sigma 5(210)$ symmetrical tilt boundary as the first attempt. One may naturally ask if the sluggish diffusion effect in this special boundary also exists in other boundaries. Although we do expect that some boundaries may show similar sluggish effects as in the $\Sigma 5(210)$ boundary, caution should be taken if one wants to generalize the diffusion behavior of this special boundary to other boundaries, because grain boundary diffusion mechanism can differ significantly from boundary to boundary. For example, one of the present authors (Farkas) recently showed that the diffusion kinetics of different grain boundaries varies dramatically in a polycrystalline Fe-Cr-Ni alloy [26]. Therefore, to fully address

this question, more systematic studies are needed in the future to investigate the diffusion mechanisms in different types of HEA grain boundaries.

5. CONCLUSIONS

This work aims to understand if sluggish diffusion can exist in the grain boundary in a model FeNiCrCoCu HEA, which doesn't show the sluggish effect in the bulk diffusion. To achieve this, this work uses molecular dynamics simulations to calculate and compare the self-diffusivities of a <100>Σ5(210) symmetric tilt grain boundary in an equiatomic FeNiCrCoCu HEA and its corresponding average atom (AA) material, the latter of which lacks the effects from compositional randomness. Different from the lack of sluggish diffusion in the bulk HEA predicted by the same interatomic potentials [12], this work shows that the sluggish diffusion is evident in this HEA model grain boundary at low temperatures but the sluggish effect diminishes as the temperature approaches the melting point. To understand the underlying reason, the atom diffusion trajectories at the grain boundary region are analyzed for both HEA and AA material. The results show that they have different diffusion mechanisms at low temperatures but similar ones at high temperatures. In particular, some atoms in the HEA grain boundary have to diffuse out of the central boundary region for continuous diffusion at low temperatures, which has a high-energy cost. In contrast, the atoms in the AA boundary mainly diffuse along the central boundary plane at low temperatures. We believe this is a result of the diffusing atoms encountering "trapping" sites in the HEA boundary, where the atoms have limited options to escape or bypass in the 2D confined space. As temperature rises, diffusion becomes viable along both in-plane and out-of-plane paths and sufficient kinetic energies are available to escape these trapping sites, resulting in the loss of sluggish diffusion at high temperatures. In the bulk HEA, the diffusion is in 3D so that atoms have

more options to escape or bypass the trapping sites. We think this may be the reason why the sluggish diffusion effect does not exist in the model bulk HEA but it occurs at the model HEA grain boundary. The results obtained here suggest that in general, the sluggish diffusion effect may be stronger in lower dimension high diffusivity paths at lower temperatures than that in the bulk HEA. However, the results of this work are only based on one special boundary. Therefore, more studies are needed to determine if the sluggish effect observed here also exists in other HEA grain boundaries.

In short, the major conclusions are summarized as follows:

- 1. The $\Sigma 5(210)$ grain boundary diffusion is slower in the HEA than in the AA, especially at low temperatures, demonstrating that grain boundary sluggish diffusion can exist in HEAs.
- 2. The trapping sites in the HEA can effectively block the grain boundary diffusion (thus induce the sluggish diffusion) at low temperatures, due to the confined 2D space of the grain boundary.
- 3. The trapping sites may not be effective for bulk diffusion (thus no sluggish diffusion), because vacancies have many other alternative paths to escape in the 3D space.
- 4. The generality of sluggish grain boundary diffusion in HEAs needs more investigations in the future.

Acknowledgements

The authors acknowledge Advanced Research Computing (ARC) at Virginia Tech for providing computational resources and technical support that have contributed to the results reported within this paper. URL: https://arc.vt.edu/.

AS acknowledges the support from Virginia Tech's Institute of Critical Technologies and Applied Sciences (ICTAS) Doctoral Scholars Program.

DF acknowledges support from the US National Science Foundation, Grant 1507846.

XMB acknowledges the support from the US National Science Foundation under Grant No. 1847780.

Author contributions

A. Seoane: Conceptualization, Methodology, Software, Formal analysis, Investigation, Writing – original draft, Visualization.

D. Farkas: Conceptualization, Methodology, Formal analysis, Writing – review & editing, Supervision, Funding acquisition.

X.M. Bai: Conceptualization, Methodology, Writing – review & editing, Supervision, Funding acquisition.

Conflicts of interest or competing interests

The authors declare they have no known conflict of interest.

Data and code availability

Data will be made available on request.

Supplementary information

Not applicable.

Ethical approval

Not applicable.

REFERENCES

- [1] Praveen S, Kim HS (2018) High-entropy alloys: potential candidates for high-temperature applications—an overview. Adv Eng Mater 20: 1700645 (1-22).
- [2] Miracle DB, Senkov ON (2017) A critical review of high entropy alloys and related concepts. Acta Mater 122: 448-511.
- [3] Yeh JW (2006) Recent progress in high entropy alloys. Ann Chim Sci Mat 31: 633-648.
- [4] Yeh JW (2015) Physical metallurgy of high-entropy alloys. JOM 67: 2254-2261.
- [5] Divinski SV, Pokoev AV, Esakkiraja N, Paul A (2018) A mystery of sluggish diffusion in high-entropy alloys: the truth or a myth? Diffusion Foundations 17: 69-104.
- [6] Dąbrowa J, Zajusz M, Kucza W, Cieślak G, Berent K, Czeppe T, Kulik T, Danielewski M (2019) Demystifying the sluggish diffusion effect in high entropy alloys. J Alloys Compd 783: 193-207.
- [7] Dąbrowa J, Danielewski M (2020) State-of-the-art diffusion studies in the high entropy alloys. Metals 10: 347 (1-44).
- [8] Daw MS, Chandross M (2021) Sluggish diffusion in random equimolar FCC alloys. Phys Rev Mater 5: 043603 (1-17).
- [9] Miracle DB (2017) High-entropy alloys: A current evaluation of founding ideas and core effects and exploring "nonlinear alloys". JOM 69: 2130-2136.
- [10] Tsai KY, Tsai MH, Yeh JW (2013) Sluggish diffusion in Co–Cr–Fe–Mn–Ni high-entropy alloys. Acta Mater 61: 4887-4897.
- [11] Cantor B, Chang ITH, Knight P, Vincent AJB (2004) Microstructural development in equiatomic multicomponent alloys. Mater Sci Eng, A 375: 213-218.
- [12] Seoane A, Farkas D, Bai X-M (2022) Influence of compositional complexity on species diffusion behavior in high-entropy solid-solution alloys. J Mater Res 37: 1403-1415.
- [13] Farkas D, Caro A (2018) Model interatomic potentials and lattice strain in a high-entropy alloy. J Mater Res 33: 3218-3225.
- [14] Varvenne C, Luque A, Nöhring WG, Curtin WA (2016) Average-atom interatomic potential for random alloys. Phys Rev B 93: 104201 (1-7).
- [15] Kaur I, Mishin Y, Gust W (1995) Fundamentals of grain and interphase boundary diffusion. 3rd ed., Wiley.
- [16] Burke J (1957) Role of Grain Boundaries in Sintering. J Am Ceram Soc 40: 80-85.

- [17] Langdon TG (1970) Grain boundary sliding as a deformation mechanism during creep. Philos Mag 22: 689-700.
- [18] Ralston K, Birbilis N (2010) Effect of grain size on corrosion: a review. Corrosion 66: 075005 (1-13).
- [19] Fisher JC (1951) Calculation of diffusion penetration curves for surface and grain boundary diffusion. J Appl Phys 22: 74-77.
- [20] Bokstein B, Rodin A (2014) Grain boundary diffusion and grain boundary segregation in metals and alloys. Diffusion Foundations 1: 99-122.
- [21] Inoue A, Nitta H, Iijima Y (2007) Grain boundary self-diffusion in high purity iron. Acta Mater 55: 5910-5916.
- [22] Smith A, Gibbs G (1969) Volume and grain-boundary diffusion in 20 Cr/25 Ni/Nb stainless steel. Met Sci J 3: 93-94.
- [23] Chen T-F, Tiwari GP, Iijima Y, Yamauchi K (2003) Volume and grain boundary diffusion of chromium in Ni-base Ni-Cr-Fe alloys. Mater Trans, JIM 44: 40-46.
- [24] Vaidya M, Pradeep KG, Murty BS, Wilde G, Divinski SV (2017) Radioactive isotopes reveal a non sluggish kinetics of grain boundary diffusion in high entropy alloys. Sci Rep 7: 12293 (1-11).
- [25] Glienke M, Vaidya M, Gururaj K, Daum L, Tas B, Rogal L, Pradeep K, Divinski SV, et al. (2020) Grain boundary diffusion in CoCrFeMnNi high entropy alloy: kinetic hints towards a phase decomposition. Acta Mater 195: 304-316.
- [26] Farkas D (2021) Varying Diffusion Kinetics Along Random Grain Boundaries in a Model Austenitic Stainless Steel. Metall Mater Trans A 52: 1117-1126.
- [27] Koju R, Mishin Y (2020) Atomistic study of grain-boundary segregation and grain-boundary diffusion in Al-Mg alloys. Acta Mater 201: 596-603.
- [28] Mendelev MI, Zhang H, Srolovitz DJ (2005) Grain boundary self-diffusion in Ni: Effect of boundary inclination. J Mater Res 20: 1146-1153.
- [29] Mishin Y, Asta M, Li J (2010) Atomistic modeling of interfaces and their impact on microstructure and properties. Acta Mater 58: 1117-1151.
- [30] Suzuki A, Mishin Y (2005) Atomic mechanisms of grain boundary diffusion: Low versus high temperatures. J Mater Sci 40: 3155-3161.

- [31] Frolov T, Olmsted DL, Asta M, Mishin Y (2013) Structural phase transformations in metallic grain boundaries. Nat Commun 4: 1-7.
- [32] Chesser I, Mishin Y (2022) Point-defect avalanches mediate grain boundary diffusion. Commun Mater 3: 90 (1-10).
- [33] Zhang H, Srolovitz DJ, Douglas JF, Warren JA (2009) Grain boundaries exhibit the dynamics of glass-forming liquids. Proc Natl Acad Sci USA 106: 7735-7740.
- [34] Bai X-M, Li M (2008) Ring-diffusion mediated homogeneous melting in the superheating regime. Phys Rev B 77: 134109 (1-13).
- [35] Plimpton S (1995) Fast Parallel Algorithms for Short-Range Molecular-Dynamics. J Comput Phys 117: 1-19.
- [36] Hoover WG (1985) Canonical dynamics: Equilibrium phase-space distributions. Phys Rev A 31: 1695-1697.
- [37] Daw MS, Baskes MI (1984) Embedded-Atom Method Derivation and Application to Impurities, Surfaces, and Other Defects in Metals. Phys Rev B 29: 6443-6453.
- [38] Pasianot R, Farkas D (2020) Atomistic modeling of dislocations in a random quinary high-entropy alloy. Comput Mater Sci 173: 109366 (1-12).
- [39] Zhang L, Shibuta Y (2020) Inverse Hall-Petch relationship of high-entropy alloy by atomistic simulation. Mater Lett 274: 128024 (1-4).
- [40] Liu J (2020) Molecular dynamic study of temperature dependence of mechanical properties and plastic inception of CoCrCuFeNi high-entropy alloy. Phys Lett A 384: 126516 (1-5).
- [41] Divinski S, Lohmann M, Herzig C (2004) Grain boundary diffusion and segregation of Bi in Cu: radiotracer measurements in B and C diffusion regimes. Acta Mater 52: 3973-3982.
- [42] Deacon CG (1992) Error analysis in the introductory physics laboratory. The Physics Teacher 30: 368-370.
- [43] Utt D, Stukowski A, Albe K (2020) Grain boundary structure and mobility in high-entropy alloys: A comparative molecular dynamics study on a Σ11 symmetrical tilt grain boundary in face-centered cubic CuNiCoFe. Acta Mater 186: 11-19.
- [44] Frolov T, Mishin Y (2009) Molecular dynamics modeling of self-diffusion along a triple junction. Phys Rev B 79: 174110 (1-5).
- [45] Stukowski A (2009) Visualization and analysis of atomistic simulation data with OVITO—the Open Visualization Tool. Modell Simul Mater Sci Eng 18: 015012 (1-7).

[46] Bai X-M, Voter AF, Hoagland RG, Nastasi M, Uberuaga BP (2010) Efficient annealing of radiation damage near grain boundaries via interstitial emission. Science 327: 1631-1634.

Graphical abstract

